sustainability

MDPI

Article

Hydrothermally Treated Cement Bypass Dust as a Supplementary Cementitious Material

Rimvydas Kaminskas *, Brigita Savickaite and Anatolijus Eisinas

Department of Silicate Technology, Faculty of Chemical Technology, Kaunas University of Technology, Radvilenu 19, LT-50254 Kaunas, Lithuania; brigita.savickaite@ktu.lt (B.S.); anatolijus.eisinas@ktu.lt (A.E.)
* Correspondence: rimvydas.kaminskas@ktu.lt; Tel.: +370-62023774

Abstract

In this study, the possibility of using cement bypass dust as a cement additive was investigated. The utilization of cement bypass dust remains a major problem in cement production, as huge amounts of it are stored in landfills. In this study, a hydrothermal treatment is proposed to modify the properties of this dust and to expand its use. Hydrothermal treatment with pure bypass dust and quartz was carried out to achieve a CaO/SiO_2 ratio of 1 to 2. Samples were synthesized at 200 °C for 2, 4, 8, and 24 h. To examine the influence of the hydrothermal treatment on cement properties, a sample with a CaO/SiO_2 ratio of 1, hydrothermally treated for 8 h, was selected. This study employed XRD, XRF, DSC-TG, and isothermal calorimetry. Most of the target synthesis products, e.g., tobermorite and calcium silicate hydrates, formed after 8 h of sample synthesis, during which quartz was added to bypass dust and a CaO/SiO_2 ratio of 1 was achieved. An examination of the composition of the liquid medium following hydrothermal processing showed that almost all chlorine passed into the liquid medium, while some K_2O remained in the solid synthesis product. The synthesized additive is an effective catalyst for the hydration of Portland cement. After a 28-day curing period, specimens incorporating modified bypass dust replacing up to 10% of the Portland cement by weight demonstrated compressive strengths comparable to, or surpassing, those of specimens composed exclusively of Portland cement.

Keywords: cement bypass dust; hydrothermal treatment; Portland cement; hydration

Academic Editors: Filipe Smith Buarque and Rafael Farrapeira

Received: 19 June 2025
Revised: 18 July 2025
Accepted: 22 July 2025
Published: 24 July 2025

Citation: Kaminskas, R.; Savickaite, B.; Eisinas, A. Hydrothermally Treated Cement Bypass Dust as a Supplementary Cementitious Material. *Sustainability* **2025**, *17*, 6757. https://doi.org/10.3390/su17156757

1. Introduction

Cement production is a crucial industrial process that plays a fundamental role in infrastructure development. However, it also generates significant environmental challenges, such as greenhouse gas emissions or the consumption of energy and non-renewable resources [1]. In addition, the cement industry generates a significant amount of waste, of which cement bypass dust (CBPD) constitutes the largest proportion. CBPD is formed when a portion of the kiln system's hot gases is removed to prevent the excessive accumulation of volatile elements such as potassium, sodium, and sulfur [2]. Although this process helps to maintain the chemical stability of the cement kiln system, it generates a substantial amount of dust that poses challenges for disposal and environmental management. CBPD is a fine, powdery by-product collected from exhaust gases during cement clinker production. It consists of calcium oxide (CaO), along with high levels of alkali, particularly K_2O, chlorides, and SO_3. These properties significantly restrict the use of cement bypass dust in cement production [3]. The sustainable management of CBPD is essential to minimize environmental impact and remains a critical issue for the cement industry. Traditional disposal

methods, such as landfilling, are unsustainable and pose long-term environmental risks. Bypass dust, which is often treated as waste, has a unit cost equivalent to 20–30% of the cost per ton of clinker production, depending on the type of cement manufacturing process used. The increased utilization of alternative fuels is likely to generate greater quantities of bypass dust that require subsequent removal [4].

Therefore, there is increasing interest in finding alternative solutions for the use of CBPD. One study examined the incorporation of CBPD as an additive in calcium aluminate cement. The findings indicated that CBPD can alter the setting time and strength development of calcium aluminate cement, suggesting potential applications in specialized construction scenarios [5]. Another investigation focused on the recycling of CBPD in the production of roof tiles. The study concluded that roof tiles containing 8% CBPD and heated at 1100 °C met ASTM standards, offering a sustainable approach to the utilization of waste from construction materials [6]. Research has also explored the thermal treatment of CBPD to enhance the formation of the clinker phase in cement production. One study revealed that minor components of CBPD, particularly potassium chloride (KCl), can facilitate the formation of belite and alite at reduced temperatures, potentially leading to energy savings and improved reaction kinetics in cement manufacturing [7]. Additionally, the combined use of CBPD and blast furnace steel slag (ACS) in producing "green" cement products has been investigated. By substituting traditional materials with CBPD and ACS in cement bricks and interlocking paving blocks, products were achieved that met the requirements of strength and durability [8]. CBPD has also been investigated for use in autoclaved silica–lime products. This investigation indicated that the binder in autoclaved products can be replaced with CBPD [9]. Other authors state that cement bypass dust successfully activates slag and achieves good strength in slag-based mortars [10].

The inclusion of small amounts (1 wt.%) of CBPD has no significant impact on the physical–mechanical properties of cement [11]. It goes without saying that the potential use of this amount of waste in cement production will not solve the waste problem. The most efficient way to use waste materials is to use them as supplementary cementitious materials (SCMs). SCMs serve an essential function within the concrete industry by enhancing structural performance and environmental sustainability through the partial substitution of Portland cement. Various materials and industrial wastes are classified as SCMs, including fly ash, granulated blast furnace slag, silica fume, and various pozzolans. Their incorporation improves the strength properties of concrete and reduces the negative environmental impact of cement production while contributing to the minimization of waste [12,13].

From an environmental perspective, carbon dioxide (CO_2) emissions are directly related to the use of SCMs. About 8% of global CO_2 emissions are generated from traditional Portland cement production, which is notorious for its large carbon footprint [14]. Conversely, the incorporation of SCMs reduces these emissions due to their lower energy requirement for production and their ability to absorb CO_2 during hydration [13]. The pozzolanic activity of these materials enables reaction with calcium hydroxide, an alkaline compound produced during cement hydration, inducing the formation of cementitious compounds. In addition to increasing the strength of the concrete, it contributes to the reduction of free Ca $(OH)_2$, further alleviating the binding of CO_2 in the environment [15]. On the other hand, SCMs can act as catalysts for cement hydration reactions. In this case, SCMs do not alter the composition of cement hydration products, but act as materials to nucleate cement hydrates and accelerate the overall cement hydration process [16]. Such materials are sometimes called microfillers. They can typically replace a smaller amount of cement clinker than active pozzolanic materials, but they enable a significantly wider range of materials to be used.

Potential supplementary cementitious materials are also purposely synthesized materials. Such materials can come in the form of calcium silicate hydrates, which act not only as catalysts for cement hydration but also improve the strength and durability of cement stone [17–20]. These properties are characteristic of both crystalline calcium silicate hydrates, such as tobermorite, gyrolite, and others, and semicrystalline or amorphous calcium silicate hydrates [21]. It could also be materials that originate from the thermal treatment of minerals and waste materials. One of these is scawtite, which, when added to Portland cement, can yield a more robust microstructure, which alters the rheological behavior of concrete mixtures and increases strength [22–24]. The ability to fill the capillary pores contributes to a denser microstructure, therefore improving durability and mechanical performance [25].

Thus, the use of cement bypass dust as secondary raw materials remains a relevant issue, and it is necessary to find new effective ways to utilize waste materials. It would be especially beneficial if it allowed the use of larger amounts of this waste. On the other hand, the heat generated during cement production is not fully utilized for all technological processes. Most of the secondary heat is used to dry raw materials, but some of this heat is simply removed. Therefore, in order to utilize the secondary heat of cement production and larger amounts of CBPD, this study explored the feasibility of treating cement bypass dust using a hydrothermal process, assessed the characteristics of the resulting material, and examined its effect on the properties of Portland cement.

2. Materials and Methods

Cement bypass dust (CBPD), collected during the cleaning of hot gases from the kiln system in the production of Portland cement clinker, along with Portland cement CEM I 42.5 N, was used. The chemical compositions of the dust and cement are presented in Table 1.

Table 1. Chemical composition of raw materials.

Component (wt.%)	CBPD	Portland Cement (OPC)
SiO_2	9.29	19.72
Al_2O_3	2.76	4.93
Fe_2O_3	2.15	3.25
CaO	47.70	61.19
MgO	1.68	3.93
K_2O	15.30	1.04
Na_2O	0.50	0.14
SO_3	6.90	2.6
P_2O_5	0.08	-
TiO_2	0.19	-
Cl	10.30	not estimated
Other	3.15	3.2
Specific surface area (m^2/kg)	420 *	320

* after additional milling.

XRD analysis data (Figure 1a) imply that CBPD contains sylvite (PDF 04-008-1875), portlandite (PDF 00-044-1481), calcium oxide (PDF 01-070-4068), larnite (PDF 00-033-0302) and potassium sulphate (PDF 00-018-1060). In the XRD curve, a hump was also observed at 25–35 2θ, typical of amorphous materials.

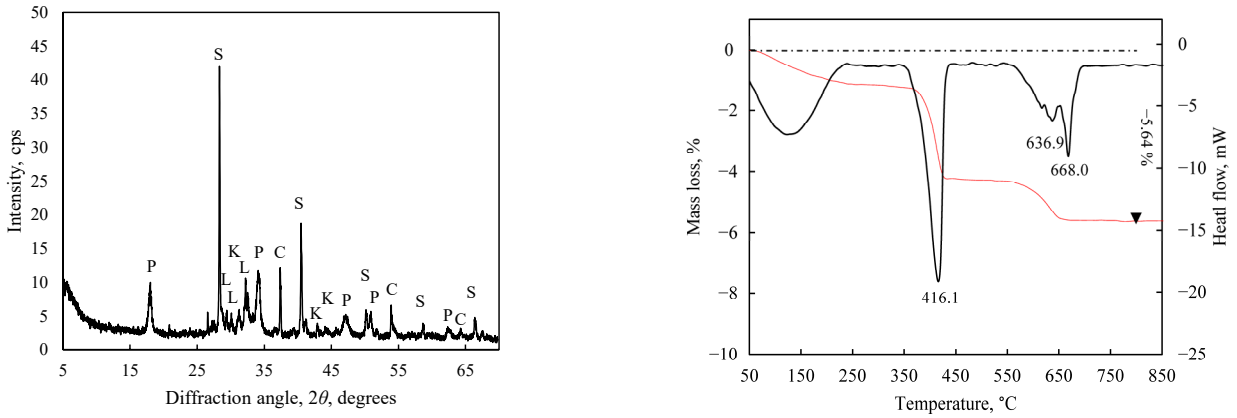

(**a**) (**b**)

Figure 1. (**a**) X-ray diffraction patterns of CBPD. Abbreviations: S, sylvite (KCl); P, portlandite ($Ca(OH)_2$); C, calcium oxide (CaO); L, larnite (Ca_2SiO_4); and K, potassium sulphate (K_2SO_4). (**b**) Simultaneous thermal analysis (red line—TG; black line—DSC) results of CBPD.

In the CBPD DSC curve (Figure 1b), the endo peak at 122 °C is related to the removal of adsorbed atmospheric moisture; the peak at 416 °C occurred due to the decomposition of portlandite, which is formed by CBPD's contact with atmospheric moisture, and the double peak at 640–670 °C shows the decay of calcite [26]. Calcite formation is analogous to portlandite formation and occurs when CaO from CBPD can adsorb atmospheric moisture, then react with atmospheric CO_2 and become ultrafine calcite with an undefined semicrystalline structure. For this reason, and because the main peaks of calcite are covered by the peaks of other compounds (mainly larnite), calcite was not identified by XRD. Thermogravimetric analysis (TGA) records a total weight loss of 5.64 wt.%, of which 2.98 wt.% is lost during portlandite decomposition, and 1.3 wt.% is lost during calcite decarbonation.

Because the collected dust has a heterogeneous granulometric composition, it was ground to a specific surface equal to 420 m^2/kg. After grinding, 90% of the CBPD powder was less than 55.67 µm in diameter, with a mean diameter of 20.29 µm (Figure 2).

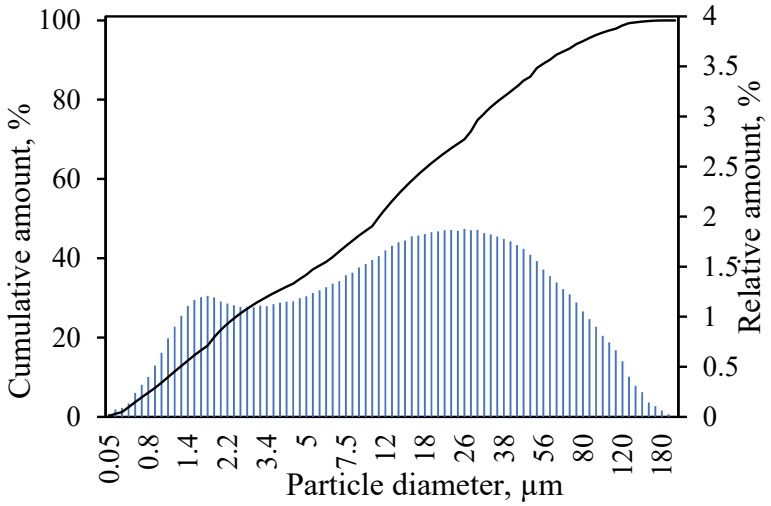

Figure 2. Particle size distribution of CBPD.

Hydrothermal treatment of CBPD: For hydrothermal synthesis, CBPD, as received and with added quartz, was selected to reach CaO/SiO_2 (C/S) ratios of 1, 1.25, 1.5, and 2.0. The abbreviations of the samples are presented in Table 2

Table 2. Sample abbreviations.

Sample	Abbreviations	C/S Ratio
CBPD	CBPD	5.13
CBPD with quartz additive	CBPD 1	1.00
	CBPD 1.2	1.2
	CBPD 1.5	1.5
	CBPD 2	2.0

Prior to synthesis, the constituents of the mixtures were precisely weighed and thoroughly homogenized using a "TURBULA TYPE T 2 F" (Willy A Bachofen AG, Muttenz, Switzerland) mixer at 49 rpm for 15 min. Each material was then mixed with deionized water with a water-to-solids ratio (W/S) of 10 (200 mL water and 20 g materials). The synthesis process was conducted without stirring in a "Parr Instruments" autoclave (Moline, IL, USA). The autoclave operated at a saturated steam temperature of 200 °C, with isothermal holding durations ranging from 2 to 24 h.

Simultaneous thermal analysis (STA) was performed using a PT1000 analyzer (Linseis Massgeraete GmbH, Selb, Germany) in a temperature range of 30–1000 °C, with a heating rate of 15 °C per minute.

X-ray diffraction (XRD) analysis was performed using a Bruker D8 Advance diffractometer (Bruker AXS GmbH, Karlsruhe, Germany) with Bragg–Brentano geometry, a detector step size of 0.02°, and a 2θ scanning range from 3° to 70°.

The X-ray fluorescence (XRF) data were collected on a Bruker S8 Tiger WD spectrometer (Bruker AXS GmbH, Karlsruhe, Germany). The data were analyzed using SPECTRAPlus V.2 QUANT EXPRESS software.

The specific surface area was measured using an automatic Blaine apparatus (TESTING Bluhm & Feuerherdt GmbH, Berlin, Germany).

The particle size distribution and specific surface area of the materials were determined using a CILAS 1090 LD particle analyzer (Cilas, Orléans, France), operating within a 0.04–500 μm range.

Properties of cement paste was ascertained according to EN 196-3 [27].

A sand-free ordinary Portland cement (OPC) paste was prepared for instrumental analysis. The samples were then immersed in distilled water at 20 ± 1 °C for 2 and 28 days. After each immersion period, the samples were crushed and rinsed with isopropyl alcohol. The material was dried at 45 °C for 12 h and subsequently stored in sealed hermetic bags.

Samples (prisms 40 × 40 × 160 mm) for compressive strength analysis were formed according to EN 196-1 [28]. The cement–sand ratio in the samples was 1:3, and the water–cement ratio was 0.5:1.

Isothermal calorimetry analysis (ICA) was performed using a TAM Air III calorimeter (TA Instruments, New Castle, DE, USA). The results were normalized to the mass of Portland cement used (per gramme).

3. Results

3.1. Hydrothermal Treatment of CBPD

Hydrothermal treatment with an isothermal sustention time at 200 °C was applied to all samples at 2, 4, 8, and 24 h. The XRD analysis curves of the samples after different durations of hydrothermal synthesis are presented in Figure 3.

It was determined that, in the pure CBPD samples, after 2 h of hydrothermal processing (Figure 3b), portlandite is formed (PDF 01-078-0315).

This sample also shows weak peaks of the CSH compound (PDF 00-033-0306) and the beginnings of the sulfate compound, cesanite (PDF 04-017-4326). Meanwhile, all samples with added quartz clearly show peaks of unreacted quartz (PDF 01-075-8320). This indicates that the isothermal holding time of 2 h is too short for the formation of crystalline calcium silicate hydrates. In addition to quartz, these samples also show characteristic peaks of cesanite, katoite (PDF 04-017-1483), calcite (PDF 01-086-4271), portlandite, and CSH.

After 4 h of hydrothermal treatment, the general trend remains unchanged, except that tobermorite (PDF 00-019-1346) begins to form in samples with a higher quartz content (lower C/S ratio) (Figure 3b, curves 2 to 4).

After 8 h of hydrothermal sustention (Figure 3c), the XRD analysis data showed significant changes in the composition of the samples, except for the CBPD sample. The composition of this sample remains the same as after 2 h of hydrothermal sustention. Meanwhile, the intensity of the unreacted quartz decreases very significantly in all samples with added quartz. At the same time, the tobermorite formed is clearly identified in all of these samples. This is especially true for CBPD 1, in which tobermorite is already the dominant phase. In addition to tobermorite, this sample also shows characteristic peaks of scawtite (PDF 00-042-1436), which is also identified in samples with a higher C/S ratio. On the other hand, only in this sample do the portlandite peaks no longer remain.

After 24 h of hydrothermal treatment (Figure 3d, curve 1), the CBPD sample consists of portlandite, cesanite, and calcium silicate hydrates. In all samples with added quartz, the peaks of the unreacted quartz still remain, the intensity of which depends on the C/S ratio in the samples: the higher the C/S ratio, the lower the peak intensity. The composition of the CBPD 1 sample remains the same as after 8 h of hydrothermal treatment. Tobermorite, scawtite, unreacted quartz, and katoite impurities are identified in this sample (Figure 3d, curve 2). In all samples with a higher C/S ratio, in addition to the main synthesis product, tobermorite, peaks of calcite, portlandite, katoite, cesanite, and calcium silicate hydrates also remain.

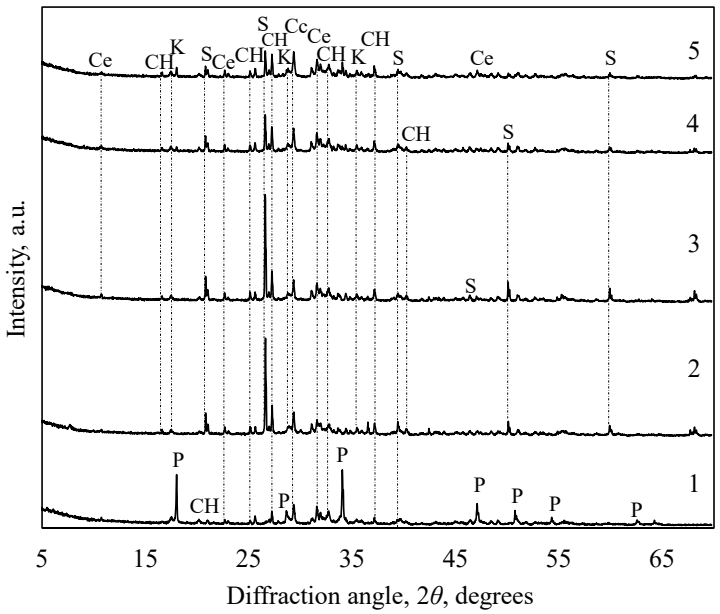

(**a**)

Figure 3. *Cont.*

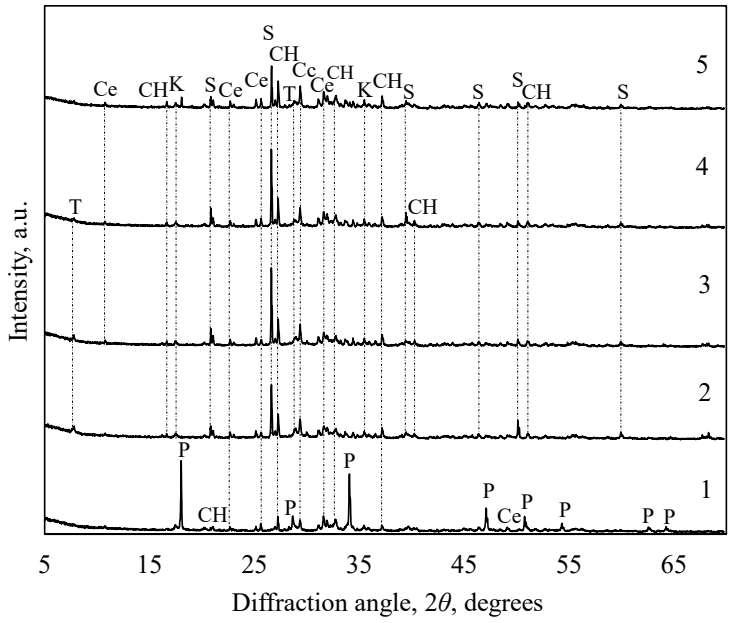

(**b**)

(**c**)

Figure 3. *Cont*.

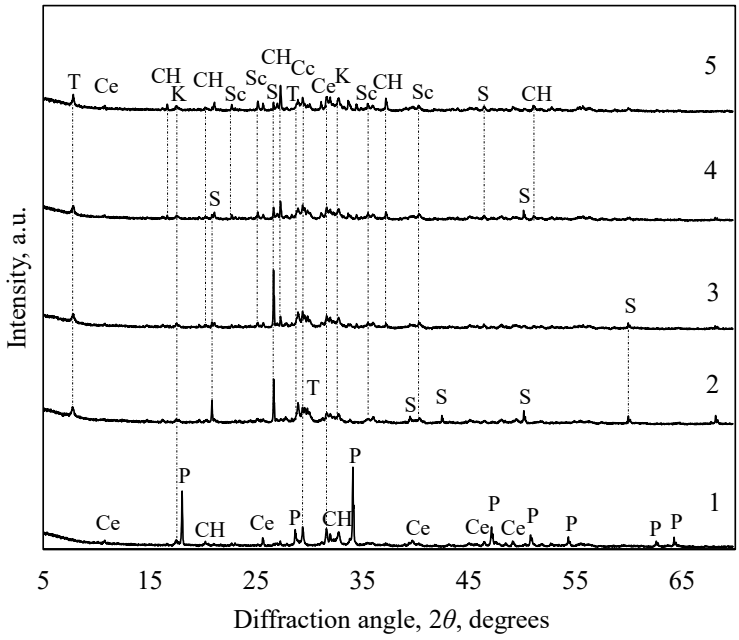

(**d**)

Figure 3. X-ray diffraction analysis of samples after hydrothermal treatment with various durations: (**a**) 2 h, (**b**) 4 h, (**c**) 8 h, and (**d**) 24 h. 1—CBPD; 2—CBPD 1; 3—CBPD 1.2; 4—CBPD 1.5; 5—CBPD 2. Abbreviations: S—quartz (SiO_2); Cc—calcite ($CaCO_3$); T—tobermorite ($Ca_5Si_6O_{16}(OH)_2 \cdot 4H_2O$); P—portlandite ($Ca(OH)_2$); K—katoite ($Ca_3Al_2(OH)_{12}$); Ce—cesanite ($Na_3Ca_2(SO_4)_3(OH)$); CH—calcium silicate hydrates; and Sc—scawtite ($Ca_7(Si_3O_9)_2CO_3 \cdot 2H_2O$).

Based on results of the XRD analysis, thermal analysis was performed for samples after 4, 8, and 24 h of hydrothermal treatment. The results of the DSC analysis are presented in Figure 4.

In the DSC (Figure 4) curves of all samples, five main endothermic effects and one exothermic effect are identified. Endothermic effects, the maximums of which are around 150, 370, 450, 573, and 750 °C, show the thermal transformation of the samples. These alterations are characteristic of the ongoing processes: The peaks at about 150 °C reflect the point at which evaporation of the bonded water occurs, while those at 450 °C reflect the point at which portlandite decomposition takes place. The peaks at ~380 °C, with a hump at ~500 °C, are assigned to the decomposition of the alumina-containing phase (C-(A) S-H), those at 573 °C reflect the recrystallization of quartz from alpha to beta modification, and those at 750 °C reflect the decomposition of $CaCO_3$ [29].

The exothermic peaks at ~810 °C appeared after 8 and 24 h of hydrothermal treatment of all samples, except for the CBPD sample; they are assigned to the crystallization of wollastonite ($CaSiO_3$) from C-S-H [30] at this temperature.

Only for the CBPD1 sample, no more portlandite remains after 8 h of hydrothermal processing. Moreover, regarding the intensities of the peaks, characteristic of the evaporation of the bonded water, and the crystallization of wollastonite, the peaks are the most intense compared to those of the other samples. Following 24 h of hydrothermal treatment, the observed trend persists; however, in the DSC profile of the CBPD1.2 sample, the peak associated with wollastonite achieves an intensity comparable to that of the CBPD1 specimen, while only minimal residual portlandite remains unreacted.

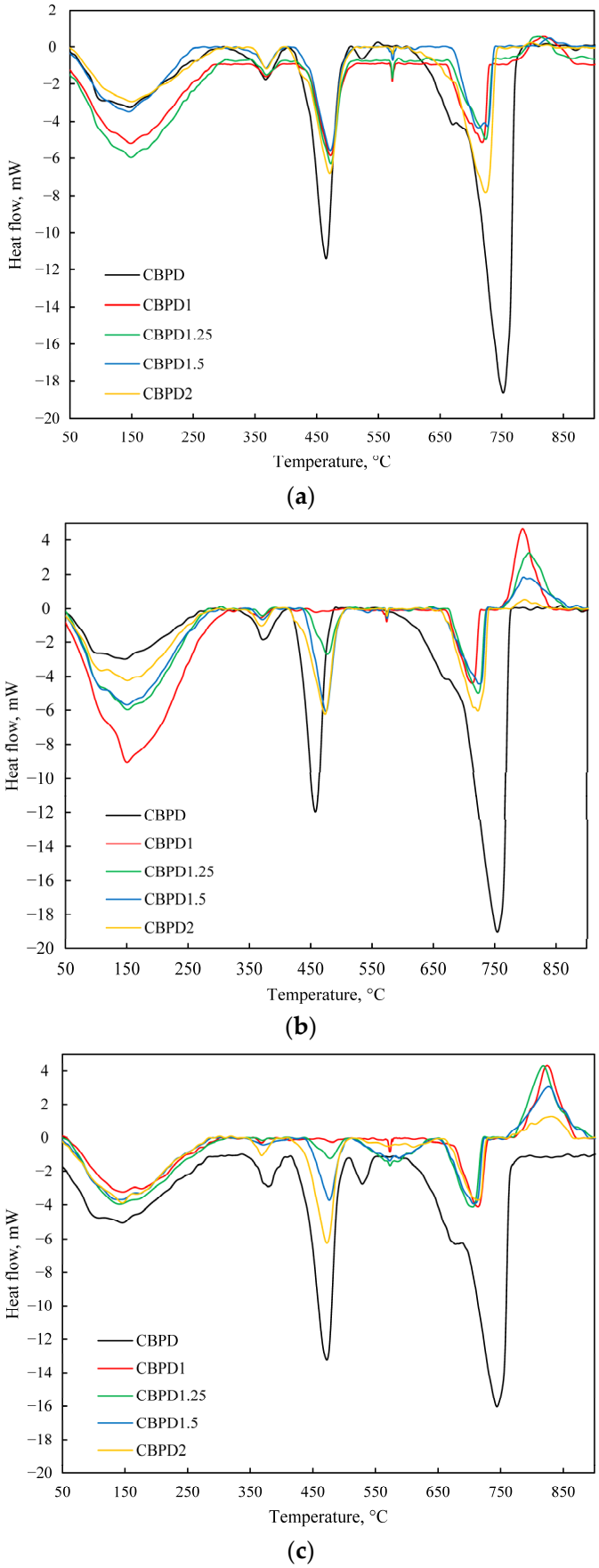

Figure 4. DSC analysis curves when the duration of hydrothermal treatment was (**a**) 4 h, (**b**) 8 h, and (**c**) 24 h.

As already mentioned, CBPD cannot return to cement production due to high levels of K_2O and chlorides. Therefore, to assess how much of these components pass into the liquid phase, the concentration of K_2O and chlorine in the liquid medium of each synthesis product was determined. The results of these studies are listed in Table 3.

Table 3. Concentration of K_2O and chlorine in the liquid medium of the synthesis product.

Concentration (wt.%) Sample	Duration of Synthesis, h							
	2	4	8	24	2	4	8	24
	K_2O				Cl			
CBPD	1.37	1.41	1.46	1.42	0.89	0.95	0.98	0.91
CBPD1	0.951	1.16	0.992	0.885	0.599	0.84	0.673	0.865
CBPD1.2	1.04	1.08	0.88	1.14	0.653	0.68	0.568	0.77
CBPD1.5	1.17	1.05	1.28	1.20	0.704	0.65	0.798	0.778
CBPD2	1.25	1.39	1.44	1.20	0.783	0.857	0.887	0.747

The concentration of both components in the liquid medium decreases as the C/S ratio of the synthesized materials decreases. This is because, due to the higher amount of quartz added, samples with a lower C/S ratio contain less K_2O and chlorine. After assessing the degree of dilution of the samples (additional quartz was added, and the water-to-solid ratio (W/S) was 10), it can be stated that almost all chlorine passes into the liquid medium, while K_2O, due to its lower solubility, remains partially in the solid synthesis product. Moreover, there is no direct relationship between the synthesis duration and the concentration of both components in the liquid medium. After only 2 h of synthesis, the majority of the K_2O and chlorine passes into the liquid medium, which changes slightly with increasing synthesis time.

To summarize the synthesis results, it can be stated that the best synthesis results are obtained by adding additional quartz to CBPD and achieving a CaO/SiO_2 ratio of 1. In this sample, most of the target synthesis products, tobermorite and calcium silicate hydrates, are formed after 8 h of synthesis. The impurities of scawtite, unreacted quartz, and katoite in this sample are not detrimental to the hydration of Portland cement [25]. Therefore, this particular sample was selected for further research, determining the influence of hydrothermally treated CBPD on the properties of Portland cement. After synthesizing a larger amount of this material, its chemical composition was determined, as presented in Table 4.

Table 4. Chemical composition of CBPD1 sample.

Component	SiO_2	CaO	Al_2O_3	SO_3	K_2O	Fe_2O_3	MgO	Cl	TiO_2	P_2O_5
Amount, (wt.%)	39.20	38.80	2.92	2.51	2.04	1.74	1.73	0.267	0.20	0.08

As can be seen from the presented data, the expected C/S ratio was maintained in the sample, and after evaluating the amount of quartz added, the K_2O concentration decreased by 6 times, while that of chlorine decreased by as much as 40 times.

3.2. Influence of Hydrothermal Treated CBPD on Portland Cement Properties

Cement paste samples were prepared by replacing 5–15 wt.% of ordinary Portland cement with the CBPD1 additive. The effect of the additive on the normal consistency and setting time of the Portland cement pastes is shown in Table 5.

Table 5. Properties of Portland cement paste with additive.

Component (wt.%)		Abbreviation	Normal Consistency W/C (%)	Setting Time (min)	
OPC	CBPD1			Initial	Final
100	-	OPC	0.28	84	136
90	5	SC5	0.29	85	145
90	10	SC10	0.30	85	150
90	15	SC15	0.30	95	155

Incorporation of the CBPD1 additive results in a marginal increase in the water required to achieve normal consistency in cement pastes. Additionally, all specimens with this additive demonstrate a modest extension in setting times compared to pure Portland cement paste, likely due to the sulphate content present in CBPD1.

Isothermal calorimetry tests were performed on a pure Portland cement sample, as well as on samples in which 5% to 15% by weight of cement was substituted with the CBPD1 additive. The results of the test are shown in Figure 5.

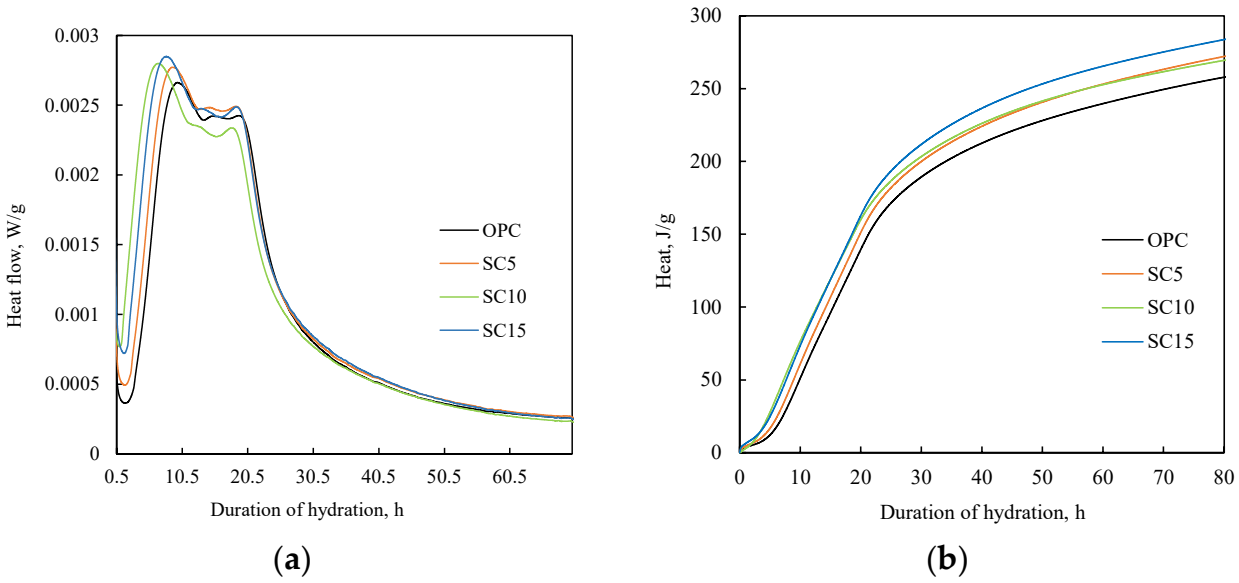

Figure 5. The ICA results of samples: (**a**) heat flow; (**b**) total heat.

The results of the ICA indicate that the CBPD1 additive catalyzes the early hydration reactions of cement. In samples with the additive, the induction period of cement hydration is significantly shortened. In the pure cement sample, this period lasts 2 h 8 min, while in the SC5 sample, it lasts 1 h 55 min; in the SC10 sample, it lasts 1 h 45 min, and in the SC15 sample, it lasts only 55 min (Figure 5a). Moreover, the second exothermic peak, associated with the hydration of calcium silicates, is manifested notably earlier in the samples incorporating the additives than in the OPC sample. Advancement of the heat flow profiles toward shorter time intervals, coupled with increased peak intensity, suggests an accelerated hydration process of calcium silicates during the initial stages. This finding is further corroborated by the increased heat of hydration observed in samples containing additives compared to the control cement sample without additives (Figure 5b). Therefore, the results of isothermal calorimetry analysis demonstrate that bypass dust hydrothermally treated with quartz additive is an effective catalyst for the early hydration of Portland cement.

The results of the XRD analysis (Figure 6) show that no new compound was formed in the samples with additive after 2 and 28 days of hardening. The difference is only noticeable

in the characteristic intensity of the peaks of unhydrated compounds and cement hydrates. After both hydration times, the portlandite peaks in the samples with the additive are more intense, whereas the peaks of the nonhydrated calcium silicates are of lower intensity than those of the OPC sample. Furthermore, in samples with 10 to 15 wt. % of the additive (Figure 6, curves 3, 4), there are insignificant peaks characteristic of tobermorite, which shows that this compound only catalyzes hydration reactions but does not interject in the composition of the hydrates.

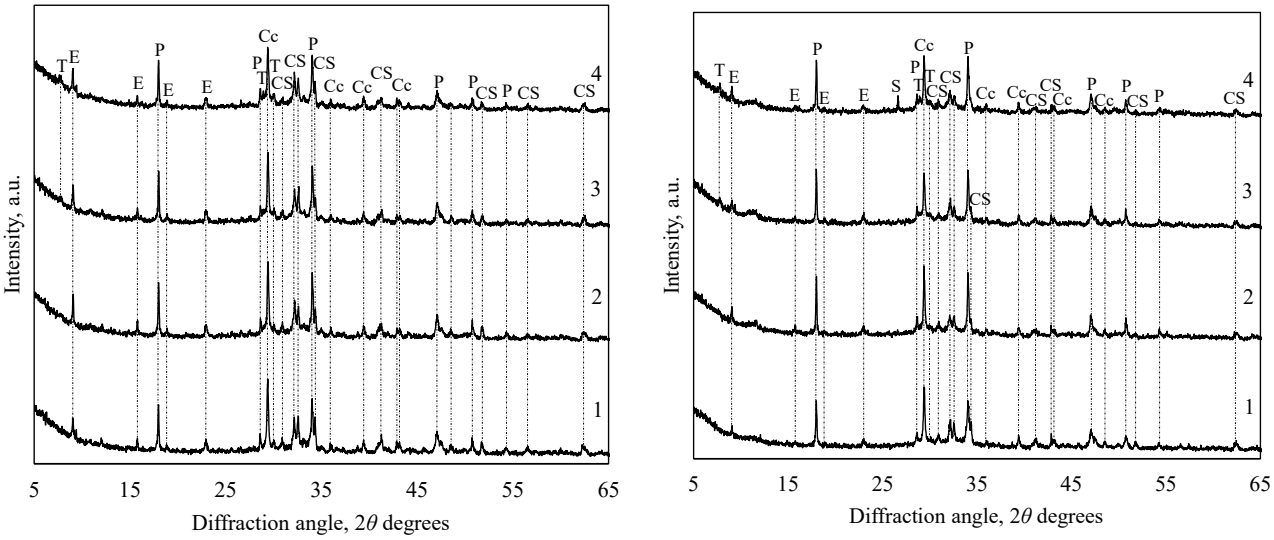

Figure 6. XRD analysis curves of the samples hydrated for 2 (**a**) and 28 (**b**) days; 1—OPC, 2—SC5, 3—SC10, and 4—SC15. Abbreviations: Cc—calcite; E—ettringite; P—portlandite; T—tobermorite; CS—calcium silicates; and S—quartz.

STA results are presented in Figure 7 and Table 6. The DSC analysis curves after 2 days of hydration (Figure 7a) are quite similar for all samples. Three endothermic peaks are observable in these curves. The peak observed between 60 and 250 °C corresponds to the decomposition of primary cement hydrates, the peak around 450 °C represents the decomposition of portlandite, and the peak between 600 and 750 °C indicates the decay of calcite [31]. The differences in the hydration process are noticeable from the results of TG analysis (Table 6). After two days of hydration, the OPC sample exhibits the greatest mass loss in the temperature range of 60 to 250 °C. In contrast, the samples containing additives show significantly higher mass losses during the decomposition of portlandite. This finding implies that, due to its structure, the CBPD1 additive promotes the formation of crystalline compounds, in our case portlandite, in the early hydration period.

After 28 days of hydration, the general trend in sample hydration remains, but with noticeable changes. The greater mass losses in the temperature range of 60 to 250 °C are already visible in the samples with additive (Table 6). This increase in mass loss is associated with the appearance of an unusual double peak in the DSC curves of samples with the additive (Figure 7b). The pure cement sample shows a peak maximum at 146 °C, whereas the samples with additives exhibit peaks at 110 °C and 156 °C. The temperature of the second peak of the double peak coincides with the peak temperature of the DSC curve of the synthesized additive (Figure 4b). Therefore, the nature of the double peak can be explained by the fact that two types of calcium silicate hydrates are formed in cement samples with additives. Conventional calcium silicate hydrates formed during cement hydration decompose at a lower temperature, 110 °C, while calcium silicate hydrates formed on the

surface of the additive acquire a crystalline structure similar to the additive and decompose at the same temperature as the additive itself, 156 °C. On the other hand, portlandite mass losses during decomposition in all additive-containing samples remain higher than those of the pure Portland cement sample. However, the fundamental difference is that the mass loss during portlandite decomposition in the OPC sample increases, whereas it decreases in samples with the additive. This cannot be explained by carbonation of the samples alone, due to the fact that the mass loss during calcite decomposition in the samples containing additives is comparable to, or lower (8–13%) than, that of the OPC sample (13%). Therefore, it can be assumed that portlandite can be adsorbed and incorporated into the crystal structure of calcium silicate hydrates [21]. Furthermore, in all DSC curves of additive-containing samples after 28 days of hydration (Figure 7b), an exothermic peak appears at a temperature of 850 to 950 °C. This peak signifies the conversion of semicrystalline or amorphous calcium silicate hydrates into wollastonite. [32]. This once again confirms that more crystalline and amorphous calcium silicate hydrates are formed in samples with additives. Notably, an increased presence of calcium silicate hydrate can enhance both the strength and durability of cementitious materials [17–20].

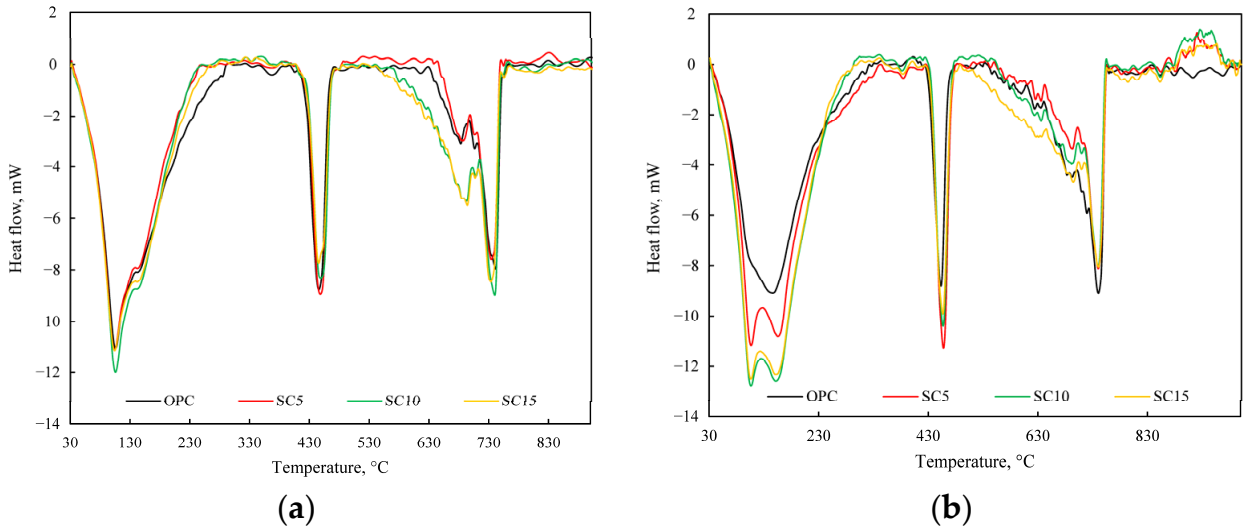

Figure 7. DSC analysis results after 2 (**a**) and 28 (**b**) days of sample hydration.

Table 6. Thermogravimetric analysis results after 2 (a) and 28 (b) days of sample hydration.

Sample	Duration (Days)					
	2			28		
	Temperature Range (°C)					
	60–250	~450	570–750	60–250	~450	570–750
	Mass Loss (%)					
OPC	8.49	1.91	7.05	10.35	1.98	8.01
SC5	8.16	2.82	5.80	11.7	2.43	6.57
SC10	8.14	2.57	6.61	10.76	2.49	7.15
SC15	8.15	2.43	6.69	10.86	2.39	7.52

Figure 8 presents the compressive strength data of the Portland cement samples at various hydration durations.

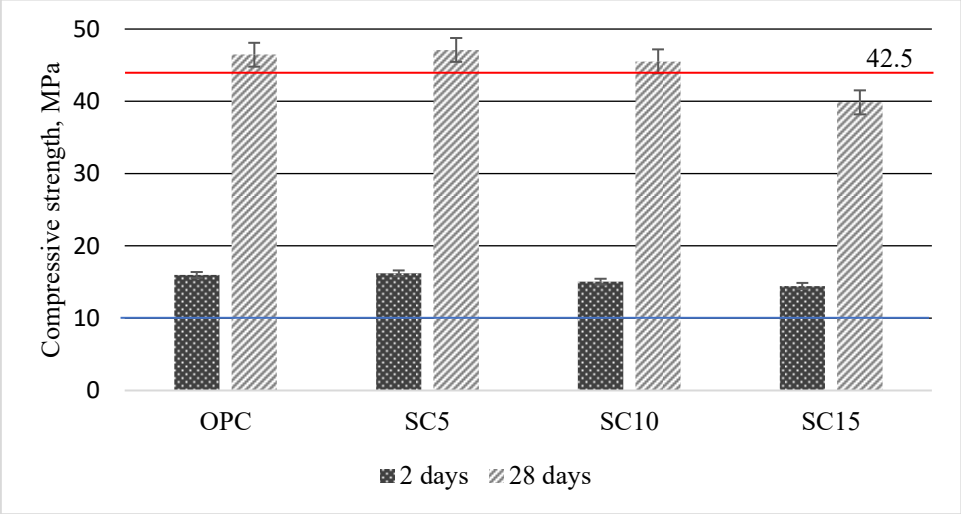

Figure 8. The compressive strength of the Portland cement samples measured after curing periods of 2 and 28 days.

After 2 days of hydration, the compressive strength of all samples is quite similar. The highest compressive strength is achieved by the SC5 sample (16.20 MPa), and the lowest value belongs to the SC15 sample (14.45 MPa). However, after 2 days of hardening, the compressive strength of all samples complies with the EN 197-1:2011 standard [33], exceeding 10 MPa. After 28 days of curing, the SC5 sample exhibited a marginally higher compressive strength (47.1 MPa) compared to the Portland cement sample (46.45 MPa), while SC10 showed a slightly lower value (45.5 MPa). The compressive strength of the SC15 sample fell below 42.5 MPa, which does not meet the 42.5 N cement standard.

In conclusion, replacing 10% of the cement by weight with hydrothermally treated bypass dust allows for sustainable reuse of a substantial amount of this waste material.

4. Conclusions

1. The bypass dust consists of sylvite, portlandite, calcium oxide, larnite, potassium sulphate, and amorphous compounds. This waste contains 15.3 and 10.3 wt. % K_2O and chlorides, respectively.
2. Optimal calcium silicate hydrate formation was achieved under hydrothermal treatment at 200 °C for 8 h, with a CaO/SiO_2 ratio of 1. This ratio was achieved by adding quartz. The synthesized materials consisted mainly of tobermorite and amorphous calcium silicate hydrates, along with minor amounts of scawtite, residual quartz, and katoite. In these samples, the K_2O concentration decreased by 6 times, and that of chlorine decreased by up to 40 times, compared to the initial bypass dust.
3. Bypass dust hydrothermally treated via quartz addition is an effective catalyst for early hydration of Portland cement and stimulates the formation of crystalline compounds. In the subsequent period of hydration, this additive promotes the formation of a complementary amount of crystalline and amorphous calcium silicate hydrates.
4. Up to 10% of the weight of Portland cement can be replaced with modified bypass dust without reducing the compressive strength class of Portland cement samples.
5. Research has shown that hydrothermal bypass dust treatment is an effective method for the wider use of this dust in cement production. In this work, the CaO/SiO_2 ratio of the waste was adjusted by adding quartz. Replacing quartz with silicon-rich waste from other industries would make the cement production industry even more sustainable, but new research in this direction is required.

Author Contributions: Conceptualization, R.K., A.E. and B.S.; methodology, R.K., A.E. and B.S.; software, A.E. and B.S.; validation, R.K., A.E. and B.S.; formal analysis, R.K. and B.S.; investigation, R.K., A.E. and B.S.; writing—original draft preparation, R.K., A.E. and B.S.; writing—review and editing, R.K.; visualization, R.K., A.E. and B.S.; supervision, R.K. All authors have read and agreed to the published version of the manuscript.

Funding: This research received no external funding.

Institutional Review Board Statement: Not applicable.

Informed Consent Statement: Not applicable.

Data Availability Statement: The data pertaining to this study are available on request from the corresponding author.

Conflicts of Interest: The authors declare no conflicts of interest.

References

1. Lang, L.; Zhu, M.; Pu, S. Recycling engineering sediment waste as sustainable subgrade material using ground granulated blast-furnace slag, electrolytic manganese residue and cement. *Environ. Techn. Innov.* **2025**, *37*, 103969. [CrossRef]
2. Wang, J.; Zeng, P.; Liu, Z.; Li, Y. Manufacture of potassium chloride from cement kiln bypass dust: An industrial implementation case for transforming waste into valuable resources. *Heliyon* **2023**, *9*, e21806. [CrossRef]
3. Popov, A.; Chernev, G. The effect of cement kiln dust on the properties of cement. *J. Chem. Technol. Metall.* **2024**, *59*, 1341–1346. [CrossRef]
4. Forinton, J. Recycling kiln bypass dust into valuable materials. In Proceedings of the CITCON 2013, Orlando, FL, USA, 11–19 April 2013; pp. 1–6. [CrossRef]
5. Nocuń-Wczelik, W.; Stolarska, K. Calorimetry in the studies of by-pass cement kiln dust as an additive to the calcium aluminate cement. *J. Therm. Anal. Calorim.* **2019**, *138*, 4561–4569. [CrossRef]
6. ElNaggar, K.A.M.; Ahmed, M.M.; Abbas, W.; Abdel Hamid, E.M. Recycling of bypass cement kiln dust in the production of eco-friendly roof tiles. *Mater. Res. Express* **2023**, *10*, 065505. [CrossRef]
7. Hanein, T.; Hayashi, Y.; Utton, C.; Nyberg, M.; Martinez, J.-C.; Quintero-Mora, N.-I.; Kinoshita, H. Pyro processing cement kiln bypass dust: Enhancing clinker phase formation. *Constr. Build. Mater.* **2020**, *259*, 120420. [CrossRef]
8. Abdel-Ghani, N.T.; El-Sayed, H.A.; El-Habak, A.A. Utilization of by-pass cement kiln dust and air-cooled blast-furnace steel slag in the production of some "green" cement products. *HBRC J.* **2018**, *14*, 408–414. [CrossRef]
9. Borek, K.; Czapik, P.; Dachowski, R. Cement Bypass Dust as an Ecological Binder Substitute in Autoclaved Silica–Lime Products. *Materials* **2023**, *16*, 316. [CrossRef]
10. Abiad, A.M.K.; Pilakoutas, K.; Guadagnini, M.; Kinoshita, H. The influence of cement bypass dust composition on the properties of slag-based mortars. *Constr. Build. Mater.* **2024**, *444*, 137829. [CrossRef]
11. Tkaczewska, E. The influence of cement bypass dust on the properties of cement curing under normal and autoclave conditions. *Struct. Environ.* **2019**, *11*, 5–22. [CrossRef]
12. Bagcal, O.; Baccay, M. Influence of agricultural waste ash as pozzolana on the physical properties and compressive strength of cement mortar. *J. Appl. Eng. Sci.* **2019**, *9*, 29–36. [CrossRef]
13. Borosnyói, A.; Kara, P.; Mlinárik, L.; Kaše, K. Performance of waste glass powder (wgp) supplementary cementitious material (scm)—workability and compressive strength. *Építőanyag* **2013**, *65*, 90–94. [CrossRef]
14. Li, Y.; Liu, Y.; Lin, H.; Jin, C. Study of flexural strength of concrete containing mineral admixtures based on machine learning. *Sci. Rep.* **2023**, *13*, 18061. [CrossRef] [PubMed]
15. Teixeira, E.; Mateus, R.; Camões, A.; Branco, F. Quality and durability properties and life-cycle assessment of high volume biomass fly ash mortar. *Constr. Build. Mater.* **2019**, *197*, 195–207. [CrossRef]
16. Nicoleau, L. Accelerated growth of calcium silicate hydrates: Experiments and simulations. *Cem. Concr. Res.* **2011**, *41*, 1339–1348. [CrossRef]
17. Alizadeh, R.; Beaudoin, J.J.; Raki, L. Mechanical properties of calcium silicate hydrates. *Mater. Struct.* **2011**, *44*, 13–28. [CrossRef]
18. Kumar, A.; Walder, B.J.; Kunhi Mohamed, A.; Hofstetter, A.; Srinivasan, B.; Rossini, A.J.; Scrivener, K.; Emsley, L.; Bowen, P. The atomic-level structure of cementitious calcium silicate hydrate. *J. Phys. Chem. C* **2017**, *121*, 17188–17196. [CrossRef]
19. Abu Bakr, M.; Singh, B.K. Strength and durability properties of recycled aggregate concrete blended with hydrated lime and brick powder. *Eur. J. Environ. Civ. Eng.* **2023**, *28*, 1259–1283. [CrossRef]
20. Miah, M.J.; Huaping, R.; Paul, S.C.; Babafemi, A.J.; Li, Y. Long-term strength and durability performance of eco-friendly concrete with supplementary cementitious materials. *Innov. Infrastruct. Solut.* **2023**, *8*, 255. [CrossRef]

21. Eisinas, A.; Baltakys, K.; Siauciunas, R. The effect of gyrolite additive on the hydration properties of Portland cement. *Cem. Concr. Res.* **2012**, *42*, 27–38. [CrossRef]
22. Qin, Y.; Qian, X.; Tao, Y.; Hu, C.; Wang, F. Unlocking the potential of dolomite for developing more sustainable cementitious materials through partial calcination. *ACS Sustain. Chem. Eng.* **2024**, *12*, 16378–16387. [CrossRef]
23. Zhang, Y.; Yang, D.; Gu, X.; Chen, H.; Li, Z. Application of iron tailings-based composite supplementary cementitious materials (SCMs) in green concrete. *Materials* **2022**, *15*, 3866. [CrossRef]
24. Pushkarova, K.; Kochevykh, M.; Honchar, O.; Hadaichuk, D. Features of hardening and utilization of modern cement compositions with nanomodifying additives for repair and restoration works. *Int. J. Conserv. Sci.* **2024**, *15*, 157–168. [CrossRef]
25. Lallas, Z.; Gombeda, M.; Mendonca, F. Review of supplementary cementitious materials with implications for age-dependent concrete properties affecting precast concrete. *PCI J.* **2023**, *68*, 46–64. [CrossRef]
26. Kang, H.; Kang, S.; Lee, B. Strength and Water-Repelling Properties of Cement Mortar Mixed with Water Repellents. *Materials* **2021**, *14*, 5407. [CrossRef] [PubMed]
27. *EN 196-3:2016*; Methods of Testing Cement. Determination of Setting Times and Soundness. Academia: Cambridge, MA, USA, 2016.
28. *EN 196-1:2016*; Methods of Testing Cement. Determination of Strength. Academia: Cambridge, MA, USA, 2016.
29. Myers, R.J.; L'Hôpital, E.; Provis, J.L.; Lothenbach, B. Effect of temperature and aluminium on calcium (alumino)silicate hydrate chemistry under equilibrium conditions. *Cem. Concr. Res.* **2015**, *68*, 83–93. [CrossRef]
30. Siauciunas, R.; Smalakys, G.; Eisinas, A.; Prichockiene, E. Synthesis of High Crystallinity 1.13 nm Tobermorite and Xonotlite from Natural Rocks, Their Properties and Application for Heat-Resistant Products. *Materials* **2022**, *15*, 3474. [CrossRef]
31. Kaminskas, R.; Monstvilaite, D.; Valanciene, V. Influence of low-pozzolanic activity calcined mica clay on hydration and hardening of Portland cement. *Adv. Cem. Res.* **2018**, *30*, 231–239. [CrossRef]
32. Gineika, A.; Siauciunas, R.; Baltakys, K. Synthesis of wollastonite from AlF3-rich silica gel and its hardening in the CO_2 atmosphere. *Sci. Rep.* **2019**, *9*, 18063. [CrossRef]
33. *EN 197-1:2011*; Cement—Part 1: Composition, Specifications and Conformity Criteria for Common Cements. iTeh, Inc.: Newark, DE, USA, 2011.